

## Measurements of radiation heat transport in germanium: Validation of an opacity model

V. J. L. White, J. M. Foster, J. C. V. Hansom, and P. A. Rosen  
*Atomic Weapons Establishment, Aldermaston, Reading RG7 4PR, United Kingdom*

S. J. Rose  
*Rutherford Appleton Laboratory, Chilton, Didcot OX11 0QX, United Kingdom*  
(Received 18 February 1994)

Measurements of radiation heat transport in germanium foils have been made to validate calculations of the radiative opacity of the heated material. Thin germanium foils were indirectly heated to a temperature of 150 eV using thermal x radiation from a laser-produced gold plasma. Emission from the rear surface of the foils was recorded using a streaked soft-x-ray imaging diagnostic, and the measured radiation-burnthrough times were compared with hydrodynamic code simulations using tabular opacities from the IMP code [S. J. Rose, *J. Phys. B* **25**, 1667 (1992)]. The IMP opacities are validated to better than  $\pm 50\%$  accuracy.

PACS number(s): 52.25.Nr, 52.50.Jm, 44.40.+a

Radiative processes play an important role in the transport of heat in high-temperature matter and may often dominate electron thermal conduction. For this reason, calculations of radiative opacity are of central importance in astrophysics and in the modeling of high-temperature laboratory plasmas. Although much of the physics underlying the calculation of radiative opacities is understood in principle, the problem is very complex and the large number of atomic electron configurations, the vast number of different possible electron transitions, and the complex dense-plasma physics which are involved make fully detailed calculations impossible for medium- and high- $Z$  elements. Different opacity models show up to factor-of-2 differences [1,2] of Rosseland-mean opacities for medium- $Z$  elements, and it is therefore important that the results of opacity calculations are tested by comparison with experimental data. Absorption-spectroscopy experiments [3–6] using radiatively heated plasmas are valuable to address particular details of the opacity calculation, but are limited to a narrow region in the spectrum and do not measure the frequency-averaged (for example, Rosseland-mean) opacity. Recently, extreme ultraviolet (xuv) absorption-spectroscopy experiments [1,7] have been carried out in the spectral region near the peak of the Rosseland weighting function, but these measurements require considerable effort if they are to provide data from which group-mean opacities may be accurately inferred and compared with model calculations. An alternative approach to testing opacity calculations is an “integrated” experiment in which the opacity is inferred by measurement of a physical quantity which is both dependent on, and sensitive to, the mean opacity.

In this paper, we present measurements of radiation-burnthrough times of germanium foils indirectly heated by thermal x radiation from a laser-produced plasma. Comparison with the results of radiation-hydrodynamic code simulations using opacities generated by the IMP [8] code are used to test the accuracy of the IMP opacity calculation.

Heat diffusion into a high-temperature, optically thick

surface is characterized by the formation of a radiation heat wave [9–12]. If the temperature  $T$  is sufficiently high for the heat front to advance supersonically then the depth of heating  $x$  varies with time  $t$  as [10]

$$x^2 \propto \frac{T^3 \lambda_R t}{\rho C_v},$$

where  $\lambda_R$  is the Rosseland mean free path and  $\rho C_v$  is the material heat capacity. The heat front is steep as a result of the strong dependence of mean free path on temperature, and for a foil of material of finite thickness the rear-surface temperature rises rapidly when the heat front reaches that surface. In principle, the Rosseland mean free path for the heated material may be determined to the same order of accuracy as the measured burnthrough time. In practice, the driving temperature may not be sufficiently high for the heat front to advance supersonically, the heated surface is ablated, and the experiment is best modeled in detail by a radiation hydrodynamic code using tabular material-property data. This is the case for the present experiment. Nevertheless, approximately the same scaling of burnthrough time with opacity is followed, and the experiment provides a sensitive test of the radiative opacities used in the hydrodynamic code calculation.

The experimental arrangement is shown schematically in Fig. 1. Thin foil samples of solid germanium were indirectly heated using thermal x radiation from a laser-produced plasma created by focusing two beams of the Atomic Weapons Establishment (AWE) HELEN Nd-glass laser onto an adjacent gold target. Each beam delivered approximately 300 J at 0.53- $\mu\text{m}$  wavelength in a 300-ps pulse. Soft-x-ray emission from the rear of the foils was detected using a streaked imaging system consisting of an imaging slit and grazing-incidence ( $15^\circ$ ) gold mirror coupled to an x-ray streak camera incorporating a thin gold-on-Parylene photocathode. The combined responses of the mirror and cathode yield a narrow spectral passband at 120-eV ( $\pm 20$ -eV) photon energy. The

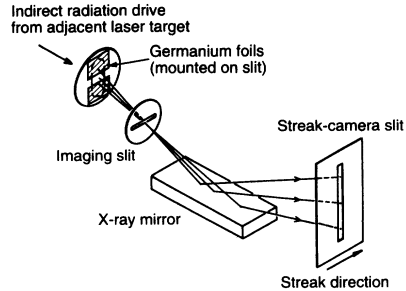


FIG. 1. Schematic of the experimental arrangement used to measure emission from the rear surface of the germanium foils.

streak camera was used at a temporal resolution of 25 ps. Typically, two germanium foils of different thickness were used, spaced a small distance apart. The gap between them allowed the streak camera to view the source of drive radiation, to provide a timing reference. The foil thicknesses used were within the range 1.7–3.4  $\mu\text{m}$  (measured to  $\pm 10\%$  accuracy). A typical streak record is shown in Fig. 2. Lineouts (Fig. 3) from each of the three regions show the temporal variation of emission (at 120 eV) from the rear surface of the foils and from the drive source. We choose to define the burnthrough time as the time between the half-peak-intensity points of the reference (drive) signal and the foil emission signal.

The choices of sample material and streak-camera spectral passband follow from several considerations. At the conditions of temperature and density achieved in the experiment medium- $Z$  elements exist in open- $M$ -shell configurations. These are treated in IMP (see below) by detailed configuration accounting together with approximate broadening models to account for clusters of satellite lines and term structure. Since radiation transport depends sensitively on windows in the opacity, this treatment is potentially inaccurate because of its implicit assumption of the merging of individual line transitions within the transition arrays: calculated opacities might in principle be in error, and the experiment addresses this point. Among candidate medium- $Z$  elements, germanium lies close to a peak in the atomic-number-dependent Rosseland-mean opacity [13]. Consequently, closest approximation to diffusive radiation transport is achieved, and the burnthrough time depends sensitively on the opacity. The 120-eV spectral passband of the streak camera was chosen to correspond to a region of high opacity

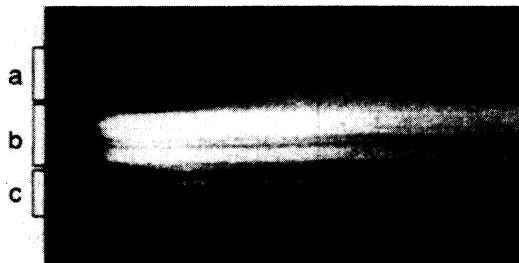


FIG. 2. Streak-camera data showing the rear-surface emission of (a) a 2.7- $\mu\text{m}$  thickness germanium foil, (b) the drive source, and (c) a 1.6- $\mu\text{m}$  thickness germanium foil.

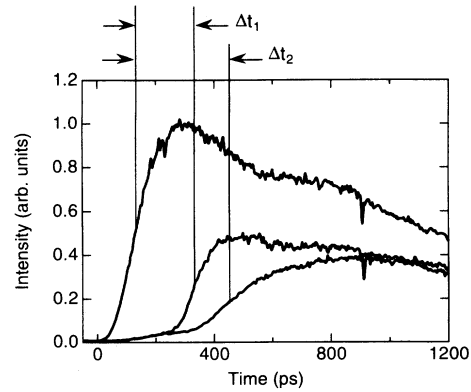


FIG. 3. Temporal variation of emission intensity from the streak record of Fig. 2.  $\Delta t_1$  and  $\Delta t_2$  are defined as the burnthrough times of the foils.

in the germanium spectrum. For material at the rear surface of the foil, the  $M$ -shell absorption edges lie below 120 eV until the time of radiation burnthrough. This contributes to steepening the rise time of the burnthrough signal, by minimizing the “escape depth” for photons from the rear surface. Finally, the gold  $M$ -band emission from the drive source lies above the germanium  $L$  absorption edges, and so contributes little radiative pre-heating.

The thermal emission from the laser-produced plasma driving the experiment was characterized using an array of filtered vacuum x-ray diodes, and the x-ray heating flux at the germanium sample is calculated from these measurements and from the geometry of the experiment. Uncertainties which result from using only a limited number of x-ray diodes to characterize the radiation drive are treated by defining minimum- and maximum-plausible drives, both of which are used in the hydrodynamic code simulations.

The experiment has been simulated in one dimension (1D) using the AWE Lagrangian radiation-hydrodynamic code NYM [14]. Radiation transport is modeled using multifrequency implicit Monte Carlo transport [15], and tabular material-property data are used (multigroup Rosseland-mean opacities from IMP, and equation-of-state data from QEOS [16]). A frequency-dependent radiation source is used in the hydrodynamic calculations to simulate the experimental radiation drive at the front surface of the foil; this is obtained from the x-ray diode data and represented by minimum- and maximum-plausible limits as discussed above. Figure 4 shows the calculated temperature and density distributions within the germanium foil, at successive 100-ps intervals, up to 1200 ps after the onset of the radiation drive. Typical material temperature and density within the bulk of the foil, at the time of burnthrough of the radiation heat wave, are 150 eV and 0.1  $\text{g cm}^{-3}$ . The hydrodynamic code simulation is post-processed to calculate emission (in the passband of the streak camera diagnostic) from the rear surface of the foil. The post-processing proceeds by integration of the equation of radiation transport through the foil, in the direction of view of the diagnostic, normal to the foil surface. Again, tab-

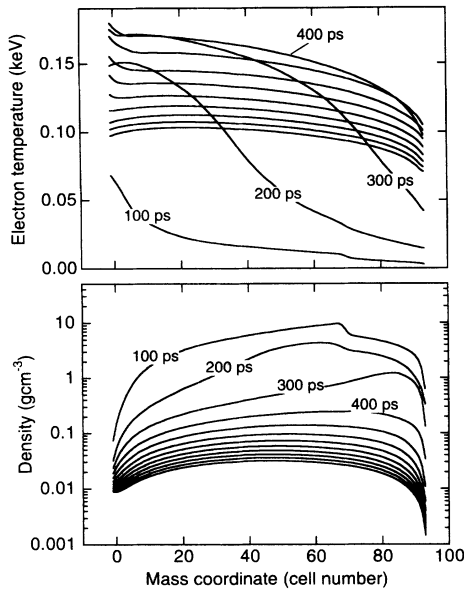


FIG. 4. Calculation temperature and density distributions within a 2- $\mu\text{m}$  original-thickness foil, at 100-ps intervals after onset of the radiation drive.

ular IMP opacity data are used. The post-processing is repeated for each output time step of the hydrodynamic code calculation, to simulate the emitted intensity as a function of time. A burnthrough time is defined in the same way as for the experimentally measured emission (time interval between the half-peak-intensity points of the drive and the rear-surface emission). This is compared with the experimental data. Figure 5 shows a comparison of the measured and calculated radiation-burnthrough times as a function of foil thickness.

To assess the importance of possible departures from local thermodynamic equilibrium (LTE), we have carried out approximate non-LTE modeling of the experiment using a scaled-hydrogenic average-atom calculation based upon the XSNQ [17] model. We take representative values of electron and radiation temperatures and material density from the hydrodynamic simulation, and use these as input to the (*post hoc*) non-LTE modeling. We calculate

the time-dependent non-LTE average-ion excitation, and compare this with the LTE excitation of the average ion under the same conditions of electron temperature and density. The difference is small, and we judge that errors which result from the use of LTE IMP opacities in our detailed simulations are insignificant in comparison with other uncertainties of the experiment.

The IMP opacity code is described in detail elsewhere [8]. In brief summary, the model starts with the solution of the Dirac equation in the Thomas-Fermi average-atom potential followed by the calculation of one- and two-electron radial integrals. All possible electron configurations (excluding those which populate the almost-empty or empty “Rydberg” shells) are constructed, and populated according to Saha-Boltzmann statistics, with configuration energies derived from the appropriate radial integrals of the wave functions. Configuration-to-configuration transition energies, together with associated oscillator strengths, are then calculated; satellite lines (resulting from spectator-electron population of the Rydberg levels) and term splitting are not included explicitly but are treated by a statistical method and represented by a Gaussian broadening of the line transitions from those configurations which are included in detail.

To explore the effect of possible errors in the IMP opacity data, we have repeated the NYM hydrodynamic code simulations and the post-processing using a simple multiplier of the opacity. This opacity multiplier is applied in the same way in the opacity data sets used for both the hydrodynamic calculation and the post-processing. A comparison of the experimental data with simulations incorporating opacity multipliers of 0.5 and 2.0 is shown in Fig 6: although the burnthrough time varies somewhat less than linearly with opacity, the scaled-opacity simulations depart significantly from experiment. In addition, we have applied the opacity multiplier separately in the hydrodynamic code and post-processing stages of the simulation. Scaled opacities have little effect in the post-processing, and an opacity multiplier of 0.5 or 2.0 results in only 10% change of burnthrough time (confirming that the rise of emission from the rear surface of the foil occurs close to the time of breakout of the radiation wave).

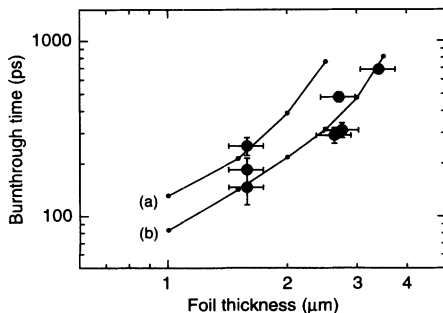


FIG. 5. Comparison of experimental burnthrough times with simulation using default IMP opacities. The curves represent the lower (a) and upper (b) plausible limits for the radiation drive used in the simulation. The data points are the experimental measurements.

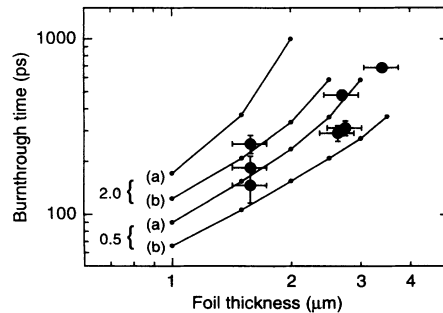


FIG. 6. Comparison of experimental burnthrough times with simulation using scaled IMP opacities. The opacity multipliers are 2.0 (upper curves) and 0.5 (lower curves). Again, (a) and (b) represent the lower and upper limits for the radiation drive.

In summary, we have described measurements of the radiation burnthrough of germanium foils indirectly heated to a peak temperature of 150 eV. The measured burnthrough times are well matched by radiation-hydrodynamic code simulations, and this comparison indicates that the IMP opacity dataset used in these calculations is in error overall by no more than 50%. The experiment demonstrates the importance of x-ray-heated

laboratory plasmas to further radiation-transport studies and the validation of radiative opacity models.

The authors would like to thank N. J. Freeman and R. T. Eagles for providing the x-ray streak camera for these experiments, and C. C. Smith, B. R. Thomas, and P. C. Thompson for helpful discussions and their continuing interest in this work.

- 
- [1] P. T. Springer, D. J. Fields, B. G. Wilson, J. K. Nash, W. H. Goldstein, C. A. Iglesias, F. J. Rogers, J. K. Swenson, M. H. Chen, A. Bar-Shalom, and R. E. Stewart, *Phys. Rev. Lett.* **69**, 3735 (1992).
  - [2] *Proceedings of the 2nd International LTE Opacity Workshop and Code Comparison Study*, edited by F. J. D. Serduke (Centre Européen de Calcul Atomique et Moléculaire, Orsay, 1991) (unpublished).
  - [3] S. J. Davidson, J. M. Foster, C. C. Smith, K. A. Warburton, and S. J. Rose, *Appl. Phys. Lett.* **52**, 847 (1988).
  - [4] J. Bruneau, C. Chenais-Popovics, D. Desenne, J.-C. Gauthier, J.-P. Geindre, M. Klapisch, J.-P. Le Breton, M. Louis-Jacquet, D. Naccache, and J.-P. Perrine, *Phys. Rev. Lett.* **65**, 1435 (1990).
  - [5] J. M. Foster, D. J. Hoarty, C. C. Smith, P. A. Rosen, S. J. Davidson, S. J. Rose, T. S. Perry, and F. J. D. Serduke, *Phys. Rev. Lett.* **67**, 3255 (1991).
  - [6] T. S. Perry, S. J. Davidson, F. J. D. Serduke, D. R. Bach, C. C. Smith, J. M. Foster, R. J. Doyas, R. A. Ward, C. A. Iglesias, F. J. Rogers, J. Abdallah, R. E. Stewart, J. D.ilkenny, and R. W. Lee, *Phys. Rev. Lett.* **67**, 3784 (1991).
  - [7] L. B. Da Silva, B. J. MacGowan, D. R. Kania, B. A. Hammel, C. A. Back, E. Hsieh, R. Doyas, C. A. Iglesias, F. J. Rogers, and R. W. Lee, *Phys. Rev. Lett.* **69**, 438 (1992).
  - [8] S. J. Rose, *J. Phys. B* **25**, 1667 (1992).
  - [9] R. E. Marshak, *Phys. Fluids* **1**, 24 (1958).
  - [10] Ya. B. Zel'dovich and Yu. P. Raizer, *Physics of Shock Waves and High-Temperature Hydrodynamic Phenomena* (Academic, New York, 1966).
  - [11] R. Sigel *et al.*, *Phys. Rev. A* **45**, 3987 (1992).
  - [12] R. Pakula and R. Sigel, *Phys. Fluids* **28**, 232 (1985).
  - [13] G. D. Tsakiris and K. Eidmann, *J. Quant. Spectrosc. Radiat. Transfer* **38**, 353 (1987).
  - [14] P. D. Roberts, Atomic Weapons Establishment Report, 1980 (unpublished).
  - [15] J. A. Fleck and J. D. Cummings, *J. Comput. Phys.* **8**, 313 (1971).
  - [16] R. M. More, K. H. Warren, D. A. Young, and G. B. Zimmerman, *Phys. Fluids* **31**, 3059 (1988).
  - [17] W. A. Lokke and W. H. Grasberger, Lawrence Livermore National Laboratory Report No. UCRL-52276, 1977 (unpublished).

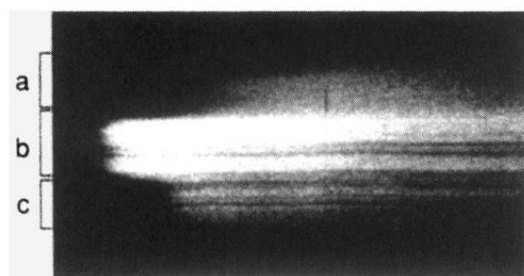


FIG. 2. Streak-camera data showing the rear-surface emission of (a) a  $2.7\text{-}\mu\text{m}$  thickness germanium foil, (b) the drive source, and (c) a  $1.6\text{-}\mu\text{m}$  thickness germanium foil.